Advances in Nano Research, *Vol. 14, No. 4 (2023) 355-362*
https://doi.org/10.12989/anr.2023.14.4.355

Application of SiO_2 nanocomposite ferroelectric material in preparation of trampoline net for physical exercise

Zhanguo Su*[1,2], Junyan Meng**[1] and Yiping Su[3]

[1]*Huainan Normal University, Huainan 232038, Anhui, China*
[2]*International College, Krirk University, Bangkok 10220, Thailand*
[3]*Faculty of Mathematics and Science, Universitity Pendidikan Sultan Idris, Malaysia*

(*Received November 2, 2021, Revised November 8, 2022, Accepted November 17, 2022*)

Abstract. Physical exercise, especially intense exercise and high intensity interval training (HIIT) by trampoline, can lead to muscle injuries. These effects can be reduced with intelligent products made of nanocomposite materials. Most of these nanocomposites are polymers reinforced with silicon dioxide, alumina, and titanium dioxide nanoparticles. This study presents a polymer nanocomposite reinforced with silica. As a result of the rapid reaction between tetraethyl orthosilicate and ammonia in the presence of citric acid and other agents, silica nanostructures were synthesized. By substituting bis (4-amino phenoxy) phenyl-triptycene in N, N-dimethylformamide with potassium carbonate, followed by catalytic reduction with hydrazine and Pd/C, the diamine monomer bis (4-amino phenoxy) phenyl-triptycene is prepared. We synthesized a new polyaromatic (imide) with triptycene unit by sol-gel method from aromatic diamines and dianhydride using pyridine as a condensation reagent in NMP. PI readily dissolves in solvents and forms robust and tough polymer films in situ. The FTIR and NMR techniques were used to determine the effects of SiO_2 on the sol-gel process and the structure of the synthesized nanocomposites. By using a simultaneous thermal analysis (DTA-TG) method, the appropriate thermal operation temperature was also determined. Through SEM analysis, the structure, shape, size, and specific surface area of pores were determined. Analysis of XRD results is used to determine how SiO_2 affects the crystallization of phases and the activation energy of crystallization.
Keywords: nanocomposite; physical exercise; PI/SiO_2; SiO_2 nanoparticles; sol-gel method

1. Introduction

Polymer composites are one of the most common types of composites. The global consumption of these composites exceeds 95% (McGrath *et al*. 1999). In organic-mineral polymer nanocomposites, one component in these structures is a mineral reinforcement (at least one dimension in a nano size), and the other is a polymer matrix. Synergistic effects between these two components determine the final properties of the nanocomposite (Ma *et al*. 2019). By combining different reinforcement types and contexts, synergistic effects may improve mechanical properties such as hardness, toughness, and electrical and optical thermal resistance (Liu *et al*. 2021, Ning *et al*. 2021, Sheng *et al*. 2021). A nanocomposite's properties are not just determined by its components' properties but also by its morphology and how its components interact (Guo *et al*. 2019). An excellent and stable nanocomposite must possess both nanoscale and microscale properties. Until the development of polymer-based composites, sports equipment primarily consisted of wood, steel, and aluminum alloys (Rasheed and Khalid 2014). Among the numerous advantages of fiber-reinforced composite materials compared to conventional materials are lightness, excellent mechanical properties, ease of design and molding, and low cost (Khalid and Chang 2022). Equipment such as tennis and squash rackets, golf sticks, fishing sticks, skis, bicycles, and skis are made from polymer-based composites (Bai and Li 2022). The extraordinary efficiency of composites has led to increased consumption of sports equipment and racing boats (Khalit *et al*. 2015).

Porous reinforcements have been introduced as a solution for problems related to nanocomposites (Delozier *et al*. 2002). Absorbent support increases the chances of polymer chains and particles engaging mechanically (Lin *et al*. 2007). Mesoporous materials such as silica can serve as reinforcement in polymeric materials (Wang *et al*. 2017). Silica aerogels, with their very high specific surface area, high porosity, and weight, are suitable for use as reinforcement materials (Dubey *et al*. 2015). The addition of silicon aerogels to polymeric surfaces increases their thermal insulation properties (Li *et al*. 2021b, Lu *et al*. 2022, Zhang *et al*. 2022c). Polyimides are high-performance macromolecules prepared by condensation polymerizing monomeric dianhydride and diamine molecules (Jin *et al*. 2012). In industrial products, these materials are used instead of glass and metals because of their high hardness and thermal and chemical resistance (Zhao *et al*. 2021, Han *et al*. 2022, Zhang *et al*. 2022b). Polyimides are used in electronic industries, tele-communication, protective coatings, and composites due to their high thermal stability (Lin *et al*. 2014). Silica nanoparticles and their surface chemistry have been investigated in this study to determine

*Corresponding author, Ph.D.,
E-mail: suzhanguo@126.com
**Co-corresponding author, Ph.D.,
E-mail: 18682969976@163.com

ISSN: 2287-237X (Print), 2287-2388 (Online)

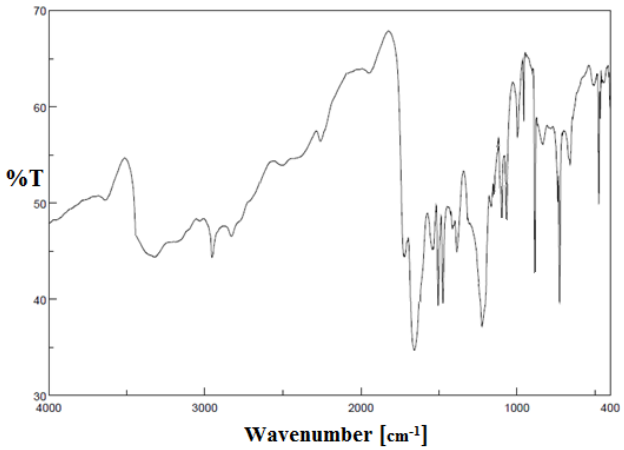

Fig. 1 Image from FT-IR of PI/SiO_2 10 wt% nanocomposite

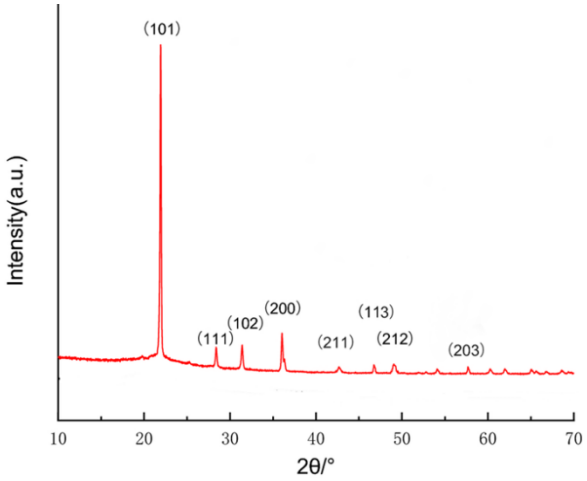

Fig. 2 SiO_2 nanoparticles X-ray

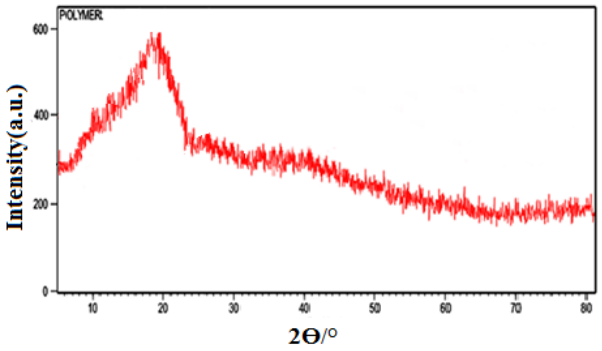

Fig. 3 Image of PI by X-ray

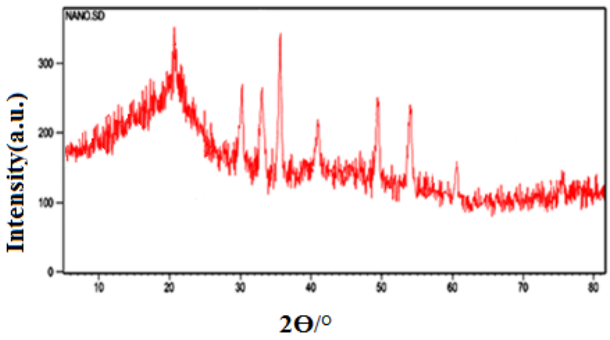

Fig. 4 Image of PI/SiO_2 10 wt% nanocomposite by X-ray

how they affect nanocomposites' properties (Babanzadeh *et al*. 2013).

A trampoline's net is easily torn by continuous jumping since they are made of polyethylene and polypropylene. As a result of torn or punctured jump nets, head injuries, knee injuries, and ankle injuries are common. Silica nanocomposites are used to produce its plates to minimize these possible damages and increase their strength, resistance, and flexibility. In this paper, a novel polyamide with aromatic dianhydride in NMP solvent and pyridine as condensing agents are synthesized and identified. Then using the sol-gel method (Rafiee 2015), new polyimide/silicate oxide composites will be synthesized. Finally, several desirable properties of PI/SiO_2 composites have attracted attention lately, such as mechanical strength, light stabilization, and antibacterial activity.

2. Results and discussion

Nanocomposite trampoline nets containing silica nanoparticles were synthesized to protect athletes from injury and increase useful life. A polyimide formed by direct condensation of 1,4-bis (4-amino phenoxy) triptycene monomer and aromatic dianhydride using acetic anhydride and pyridine as condensing reagents (Li *et al*. 2021a, 2022, Si *et al*. 2021, Wang *et al*. 2022, Zhang *et al*. 2022a, Zhao *et al*. 2022, Cao *et al*. 2023). Using NMP solvent, 86% yield was obtained. An FT-IR diagnostic method was used for identifying and diagnosing polyimide's chemical composition. The peaks appear at 1735 cm^{-1} (asymmetric C=O stretching vibration), 1728 cm^{-1} (symmetric C=O stretching vibration), 1371 cm^{-1} (C-N stretching vibration), 1222 cm^{-1} (C-O-C stretching vibration), and 728 cm^{-1} (modification of the imide ring), verifying the presence of the imide group. Also, the vibrational bands in the region of 1285 cm^{-1} are emitted by the Si-O-Si band, which indicates that silicate nanoparticles are present in the polymer tissue (Fig. 1).

A series of X-ray diffraction analyses were conducted on pure PI, pure SiO_2-NPs, and PI/SiO_2 nanocomposites, as shown in Figs. 2-4. Results indicate that PI is entirely amorphous, lacking sharp peaks in diffraction. The diffraction peaks in XRD patterns of SiO_2 powder have been indexed to the hexagonal wurtzite structure. According to Fig. 4, PI/SiO_2 nanocomposite with a ten wt% SiO_2 content displays peaks at 22°, 28°, and 36° associated with SiO_2's (101), (111), and (200) crystallines. Compared with XRD analysis of pure SiO_2 with that of a 10% nanocomposite, the spectrum of the 10% nanocomposite does not show any crystallized areas. In this case, SiO_2 is produced as an amorphous state in the sol-gel nanocomposite.

Scherrer's equation can be used to calculate average particle size. Scherrer's equation accurately calculates the average particle size to be 80 nm, which matches the value observed in the SEM image. The morphology of PI/SiO_2

Table 1 An analysis of the thermal properties of pure PI as well as PI/SiO_2 nanocomposites

Sample	PI	PI/5%SiO_2	PI/10%SiO_2
T_5[a]	243	310	323
T_{10}[b]	289	363	389
Char Yield	30	26	19
LOI	29.5	27.9	24.1

[a]Under nitrogen atmosphere, at 10°C min-1, 5% weight loss was recorded by TGA.
[b]Under nitrogen atmosphere, at 10°C min-1, 10% weight loss was recorded by TGA.

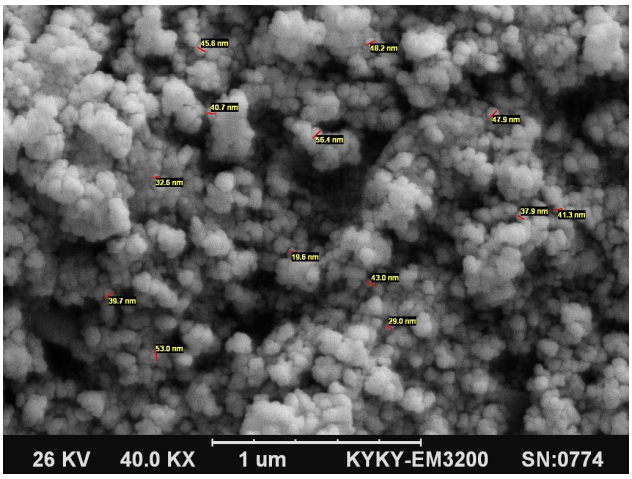

Fig. 5 Nanocomposite of PI/SiO_2 5 wt% imaged using FE-SEM

nanocomposite (5 wt%) determined by FE-SEM micrographs is shown in Fig. 5. In the photograph, there is no evidence of particle aggregation. A homogeneous dispersion of SiO_2-NPs in the PI matrix was confirmed by this image (average particle size 80 nm).

Under a nitrogen atmosphere, TGA equipment was used to study the thermal properties of pure PI and PI/SiO_2 nanocomposites at 5 and 10 wt%.and the results are shown in Fig. 6. A summary of the thermolysis results for these samples can be found in Table 1. Thermal stability studies have shown that the nanocomposites can withstand temperatures up to 300 °C. In PI and PI/SiO_2 nanocomposites with a 5 and 10 wt% weight loss, the 10 % weight loss temperature was recorded at 289, 363, and 389 °C. At 800°C, these nanocomposites' residues (char yields) exceeded 17. The thermal stability of the resulting nanocomposites is higher than pure PAI due to the excellent compatibility of polymer matrix with SiO_2 nanoparticles have high thermal stability due to their large surface area, so the incorporation of these nanoparticles can improve the thermal resistance of nanocomposites.

3. Experimental

3.1 Materials

We used chemical companies, Merck and Aldrich, to supply all reactants and did not purify them before we used them.

3.2 Techniques

A Bruker Avance 400 MHz spectrometer was used to record proton-nuclear magnetic resonance (^{1}H NMR) spectra, and proton resonances were identified as singlets (s) and multiplets (m). With a Jasco-680 (Japan) spectrophotometer, FT-IR products were recorded in KBr powder in the range of 400 to 400 cm^{-1}. A Bruker D8 Advance diffractometer was used to record the X-ray diffraction patterns of related materials. STA503 win TA is used for thermal gravimetric analysis (TGA) at a temperature of 25 to 800 °C under a nitrogen atmosphere with a heating rate of 10 °C/min.

3.3 An overview of monomer synthesis

3.3.1 A novel method for synthesizing triptycene benzoquinone

Triptycene benzoquinone 3 precipitation was prepared at 130 °C by reacting 1.1 g (1.113 x 10^{-2} mol) anthracene 1 with 1.334 g (1.23 x 10^{-10} mol) benzoquinone 2 for 3 hours. The black precipitate formed on the filter paper was washed with hot distilled water to remove excess benzoquinone after reflux. During recrystallization, yellow crystals were obtained (Scheme 1).

3.3.2 A method for synthesizing 1,4-dihydroxy-triptycene precipitate (4)

Under a temperature of 110 °C, the sediment obtained from the previous step (3) was refluxed with acetic acid solvent for four hours. A few drops of hydrobromic acid were added to the balloon after the reflux. As the solution cooled, it was poured into a beaker containing distilled water, and a white precipitate was obtained (Scheme 2).

3.3.3 Obtaining 1,4-dinitrophenoxytriptycene (6) as a monomer

A reaction mixture of 0.5 g (1.74 x 10^{-3} mol) precipitate 4 and 6 ml DMF with 0.550 g (3.51 x 10^{-3} mol) para-chloronitrobenzene 5 was added to the reaction mixture and refluxed. Following complete dissolution, 0.530 g (3.8 x 10^{-3} mol) of potassium carbonate was added to the reaction mixture at 130 °C and allowed to reflux for 8 hours. Green precipitates occur after the cooled solution of the reaction mixture is poured into a beaker containing distilled water (Scheme 3).

3.3.4 An efficient method for synthesizing bis (4aminophenoxy) phenyl triptycene

This experiment consisted of adding 0.5 g (9.4 x 10^{-4} mol) of precipitate 6, 0.05g of palladium/carbon catalyst, and 20ml of ethanol to a round-bottomed flask with a volume of 100 ml. 12 hours were spent refluxing the reaction mixture in an oil bath at 60 °C. During the reflux, 8 ml of hydrazine hydrate was added to the balloon mixture. Adding 12 ml of THF to the solution after 12 hours of reflux completed the reaction. Hot filtration was used to separate palladium and carbon from the resulting solution. As a result, yellow

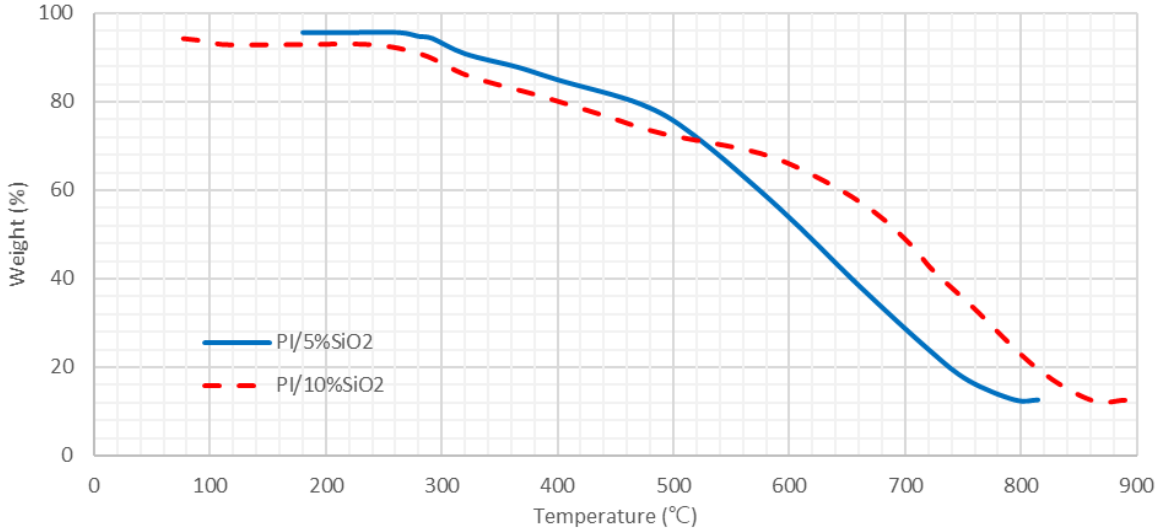

Fig. 6 An image of PI/SiO_2 nanocomposites (4 and 10 wt %) taken with a TGA

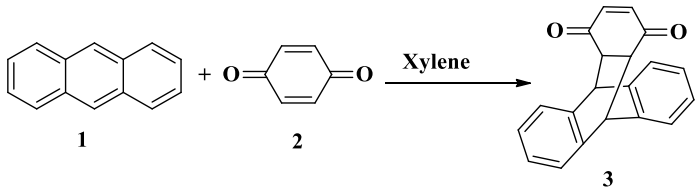

Scheme 1 A novel method for synthesizing triptycene benzoquinone

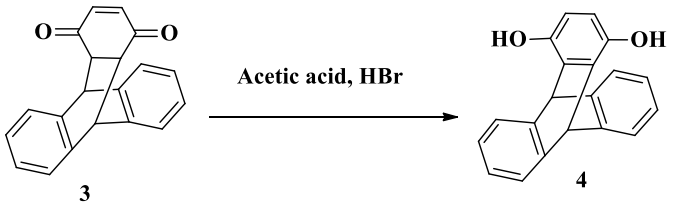

Scheme 2 A method for synthesizing 1,4-dihydroxytriptycene precipitate

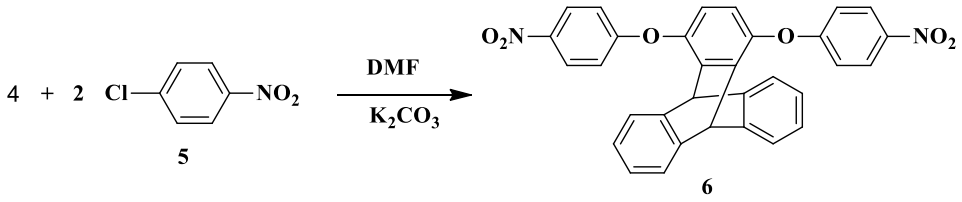

Scheme 3 Obtaining 1,4-dinitrophenoxytriptycene as a monomer

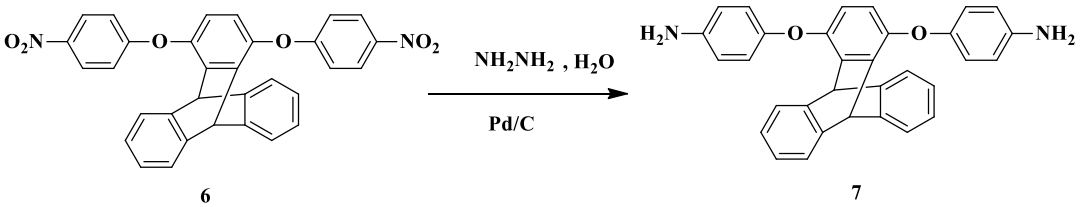

Scheme 4 An efficient method for synthesizing bis (4aminophenoxy) phenyl triptycene

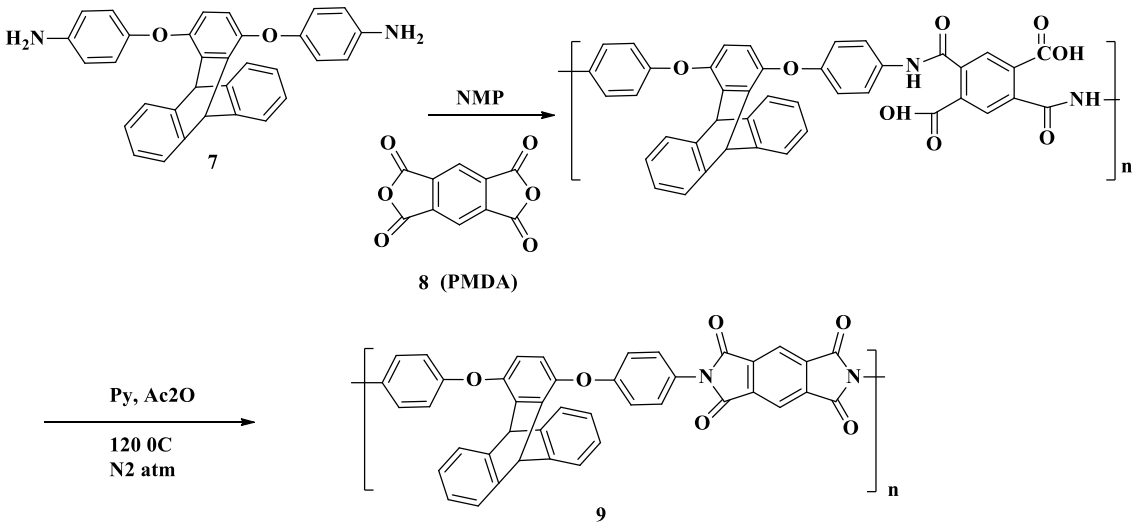

Scheme 5 Using compression polymerization to prepare polyimides

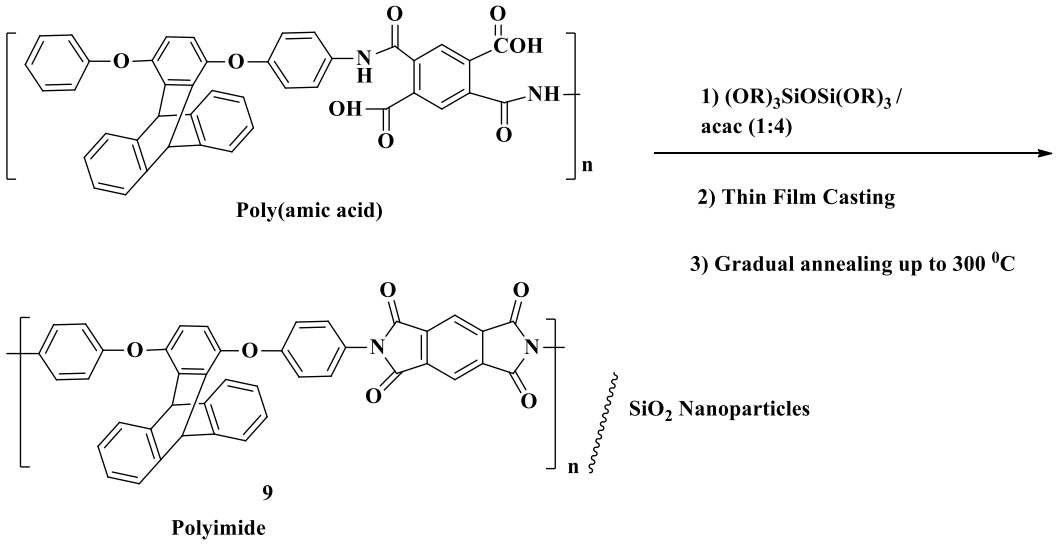

Scheme 6 A sol-gel method for preparing PI/SiO_2 nanocomposites

crystals (7) are obtained (Scheme 4) with a melting point of 204 °C and a weight of 0.28 grams (equivalent to 65%).

3.4 Using compression polymerization to prepare polyimides

Add 0.0465 g (0.2 x 10^{-4} mol) pyromellitic dianhydride 8 (PMDA) to a 25 ml round-bottomed flask, along with 0.1 g (1.2 x 10^{-4} mol) diamine monomer 7 and 2 ml NMP. In a glass container, one ml of acetic anhydride and 0.5 ml of pyridine were mixed and added to the reaction mixture at room temperature for 2 hours under a nitrogen atmosphere. During the three-hour reaction, the mixture was heated to 120°C. At room temperature, 50 ml of methanol were added to the flask's contents after cooling. As soon as the precipitates had formed, they were washed with 30 ml of methanol, followed by 90 ml of hot distilled water, and dried. The polyimide produced had a weight of 0.123, an efficiency of 86%, and a light brown color (Scheme 5).

3.5 Making SiO_2 nanoparticles

Alcohol and ammonia are mixed with water, and alkoxysilane is mixed with the rest of the alcohol. By mixing these two different solutions, the system becomes homogeneous. The molar ratios used in synthesizing these particles determine the time of hydrolysis and condensation. Hydrolysis of the alkoxysilane in an aqueous medium occurs after preparing this solution. According to this reaction, the carboxyl group replaces the hydroxyl group (Omidi *et al*. 2013, Ebrahimi and Shafiei 2017, Ehyaei *et al*. 2017, Shafiei *et al*. 2019).

3.6 A sol-gel method for preparing PI/SiO_2 nanocomposites

Equivalent molar ratios of diamine and dianhydride were dissolved in DMF. Two hours of reaction were conducted at room temperature to produce poly (amic acid).

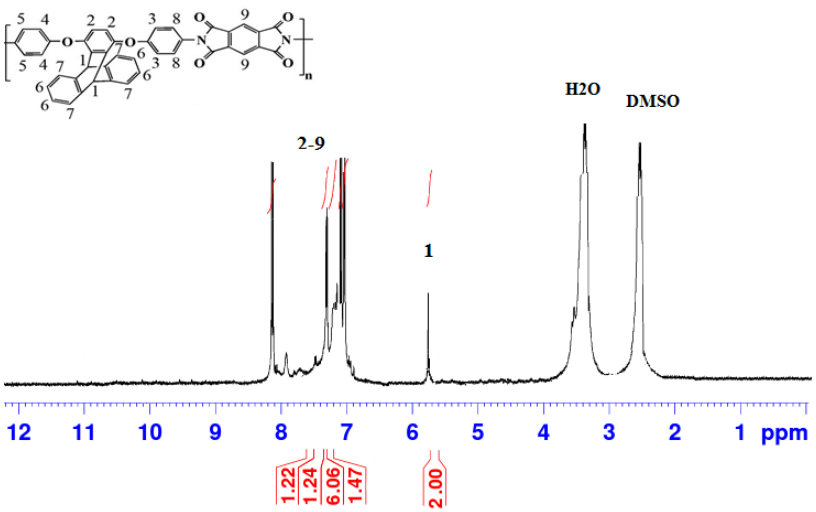

Fig. 7 PI/SiO_2 ^{1}H NMR spectrum

The poly (amic acid) solution was then stirred for 12 hours with silica nanoparticles added. For polymer and SiO_2 beds, weight ratios of 5%, 10%, 15%, and 20% are used (Scheme 6).

4. Conclusions

New aromatic polyimides bearing pendent triptycene groups were successfully synthesized with high purity and good yields. With the aid of sol-gel synthesis, PI/SiO_2 nanocomposites were successfully synthesized to improve the properties of flexibility and strength and eliminate damage caused by the tearing of trampoline nets. Nano-composites of PI/SiO_2 were successfully synthesized using sol-gel technology. FT-IR spectroscopic studies proved the utilization of poly (amic acid) and the simultaneous formation of SiO_2 nanoparticles from the hydrolysis of its precursor. FT-IR spectra confirmed Si-O-Si bonding, and SiO_2 presence in the matrix was confirmed. As the percentage of silica increases in the nanocomposites, the charring efficiency increases. XRD confirmed the amorphous nature of the silica nanoparticles. Nanoparticles of SiO_2 were uniformly dispersed within the macromolecule matrix of NCs, as revealed by SEM (Ghadiri *et al*. 2016, Ebrahimi *et al*. 2017, Mirjavadi *et al*. 2017a, b).

5. Supporting information

5.1 Experimental section

5.1.1 The general method of PI/SiO2 NC film synthesis using sol-gel

PI was synthesized by adding diamine to synthesized dianhydride, NMP, and pyridine and refluxing at 120°C under nitrogen pressure for two hours. Finally, methanol was added to the viscous mixture and stirred for 3 hours at room temperature by a magnetic stirrer. After receiving the sediment, it was washed with hot water and dried. Polyimide was mixed with silica nanoparticles in proportions of 2, 4, 6, 8, and 10, and then DMF was added. Following 12 hours of stirring, the solvent was removed, and the sediment was put in a 300-degree oven for two hours (Shafiei *et al*. 2016a, Shafiei *et al*. 2016b, Mirjavadi *et al*. 2017c, Mousavi *et al*. 2017).

5.2 Analyses of the IR spectrum, 1H NMR spectrum, and C

5.2.1 Poly imide

Brown powder, M.P: 345 °C, decompose: 1475, 1507 (C=C, Ar), 1089, 1222 (C-O-C), 1371 (C-N), 2918 (C–H, sp^2stretch), 1735, 1728 (C=O imide), IR (KBr) (νmax/cm^{-1})

^{1}H NMR, δ (ppm): 5.7 (s, 2H), 6.9-8.35(m, 9H), (400 MHz, DMSO-d6). Fig. 7.

5.2.2 SiO_2 nanoparticle 3.5 Making SiO_2 nanoparticles

White powder: 1285(Si-O-Si bond), 879 (bending mode Si–OH), IR (KBr) (νmax/cm^{-1}).

Acknowledgement

This work was supported by the research program of key scientific of the second batch of Industry-University-Research Collaborative Education Project of Ministry of Education of China in 2021, Project No. 202102205004. Anhui Provincial School-Enterprise Cooperation Practice Education Base Project, (2021xqhzsjjd075); Education and Teaching Reform Research Project, Huainan Normal University, No. 2021HSJYXM04; Teaching Research Project of Anhui Province, Based on Integrated Physical Education Professional Quality Evaluation positioning and evaluation point research.

References

Babanzadeh, S., Mehdipour-Ataei, S. and Mahjoub, A.R. (2013), "Effect of nanosilica on the dielectric properties and thermal stability of polyimide/SiO_2 nanohybrid", *Des. Monomer.*

Polym., **16**(5), 417-424. https://doi.org/10.1080/15685551.2012.747159.

Bai, H. and Li, Q. (2022), "Electrodeposited Ni/TiN-SiC nanocomposites on the dumbbell: Reducing sport injuries", *Coatings*, **12**(2), 177. https://doi.org/10.3390/coatings12020177.

Cao, Z., Niu, B., Zong, G. and Xu, N. (2023), "Small-gain technique-based adaptive output constrained control design of switched networked nonlinear systems via event-triggered communications", *Nonlinear Anal. Hybrid Syst*., **47**, 101299. https://doi.org/10.1016/j.nahs.2022.101299.

Delozier, D.M., Orwoll, R.A., Cahoon, J.F., Johnston, N.J., Smith, J.G. and Connell, J.W. (2002), "Preparation and characterization of polyimide/organoclay nanocomposites", *Polymer*, **43**(3), 813-822. https://doi.org/10.1016/S0032-3861(01)00640-1.

Dubey, R.S., Rajesh, Y.B.R.D. and More, M.A. (2015), "Synthesis and Characterization of SiO_2 Nanoparticles via Sol-gel Method for Industrial Applications", *Mater. Today*., **2**(4), 3575-3579. https://doi.org/10.1016/j.matpr.2015.07.098.

Ebrahimi, F. and Shafiei, N. (2017), "Influence of initial shear stress on the vibration behavior of single-layered graphene sheets embedded in an elastic medium based on Reddy's higher-order shear deformation plate theory", *Mech. Adv. Mater. Struct*., **24**(9), 761-772. https://doi.org/10.1080/15376494.2016.1196781.

Ebrahimi, F., Shafiei, N., Kazemi, M. and Mousavi Abdollahi, S.M. (2017), "Thermo-mechanical vibration analysis of rotating nonlocal nanoplates applying generalized differential quadrature method", *Mech. Adv. Mater. Struct*., **24**(15), 1257-1273. https://doi.org/10.1080/15376494.2016.1227499.

Ehyaei, J., Akbarshahi, A. and Shafiei, N. (2017), "Influence of porosity and axial preload on vibration behavior of rotating FG nanobeam", *Adv. Nano Res*., **5**(2), 141. https://doi.org/10.12989/anr.2017.5.2.141.

Ghadiri, M., Hosseini, S.H.S. and Shafiei, N. (2016), "A power series for vibration of a rotating nanobeam with considering thermal effect", *Mech. Adv. Mater. Struct*., **23**(12), 1414-1420. https://doi.org/10.1080/15376494.2015.1091527.

Guo, Y., Lyu, Z., Yang, X., Lu, Y., Ruan, K., Wu, Y., Kong, J. and Gu, J. (2019), "Enhanced thermal conductivities and decreased thermal resistances of functionalized boron nitride/polyimide composites", *Compos. Part B Eng*., **164**, 732-739. https://doi.org/10.1016/j.compositesb.2019.01.099.

Han, M.C., He, H.W., Kong, W.K., Dong, K., Wang, B.Y., Yan, X., Wang, L.M. and Ning, X. (2022), "High-performance electret and antibacterial polypropylene meltblown nonwoven materials doped with boehmite and ZnO nanoparticles for air filtration", *Fiber. Polym*., **23**(7), 1947-1955. https://doi.org/10.1007/s12221-022-4786-8.

Jin, L.M., Yu, S.L., Shi, W.X., Yi, X.S., Sun, N., Ge, Y.L. and Ma, C. (2012), "Synthesis of a novel composite nanofiltration membrane incorporated SiO_2 nanoparticles for oily wastewater desalination", *Polymer*, **53**(23), 5295-5303. https://doi.org/10.1016/j.polymer.2012.09.014.

Khalid, M.A.U. and Chang, S.H. (2022), "Flexible strain sensors for wearable applications fabricated using novel functional nanocomposites: A review", *Compos. Struct*., **284**, 115214. https://doi.org/10.1016/j.compstruct.2022.115214.

Khalit, M.I.B., Anuar, H.B. and Shaffiar, N.M. (2015), "Flexing test of HDPE/EPR filled CNT radiated nanocomposites for sport shoe soles", *Mater. Test*., **57**(10), 904-908. https://doi.org/10.3139/120.110786.

Li, P., Yang, M. and Wu, Q. (2021a), "Confidence interval based distributionally robust real-time economic dispatch approach considering wind power accommodation risk", *IEEE T. Sust. Energy*, **12**(1), 58-69. https://doi.org/10.1109/TSTE.2020.2978634.

Li, Y., Niu, B., Zong, G., Zhao, J. and Zhao, X. (2022), "Command filter-based adaptive neural finite-time control for stochastic nonlinear systems with time-varying full-state constraints and asymmetric input saturation", *Int. J. Syst. Sci*., **53**(1), 199-221. https://doi.org/10.1080/00207721.2021.1943562.

Li, Z.W., He, X., Zhang, C.L., Zhang, S.J., Feng, S.M., Wang, X.C., Yu, R.C. and Jin, C.Q. (2021b), "Superconductivity above 200 K observed in superhydrides of calcium", *Nature Commun*., **13**(1), 2863. https://doi.org/10.1038/s41467-022-30454-w.

Lin, C.H., Feng, C.C. and Hwang, T.Y. (2007), "Preparation, thermal properties, morphology, and microstructure of phosphorus-containing epoxy/SiO_2 and polyimide/SiO^2 nano-composites", *Eur. Polym. J*., **43**(3), 725-742. https://doi.org/10.1016/j.eurpolymj.2006.12.030.

Lin, J., Liu, Y., Yang, W., Xie, Z., Zhang, P., Li, X., Lin, H., Chen, G. and Lei, Q. (2014), "Structure and mechanical properties of the hybrid films of well dispersed SiO_2 nanoparticle in polyimide (PI/SiO2) prepared by sol–gel process", *J. Polym. Res*., **21**(8), 531. https://doi.org/10.1007/s10965-014-0531-3.

Liu, W., Zheng, Y., Wang, Z., Wang, Z., Yang, J., Chen, M., Qi, M., Ur Rehman, S., Shum, P.P., Zhu, L. and Wei, L. (2021), "Ultrasensitive exhaled breath sensors based on anti-resonant hollow core fiber with in situ grown ZnO-Bi2O3 nanosheets", *Adv. Mater. Interf*., **8**(6), 2001978. https://doi.org/10.1002/admi.202001978.

Lu, T., Yan, W., Feng, G., Luo, X., Hu, Y., Guo, J., Yu, Z., Zhao, Z. and Ding, S. (2022), "Singlet oxygen-promoted one-pot synthesis of highly ordered mesoporous silica materials via the radical route", *Green Chem*., **24**(12), 4778-4782. https://doi.org/10.1039/D2GC00869F.

Ma, P., Dai, C., Wang, H., Li, Z., Liu, H., Li, W. and Yang, C. (2019), "A review on high temperature resistant polyimide films: Heterocyclic structures and nanocomposites", *Compos. Commun*., **16**, 84-93. https://doi.org/10.1016/j.coco.2019.08.011.

McGrath, J.E., Dunson, D.L., Mecham, S.J. and Hedrick, J.L. (1999), *Synthesis and Characterization of Segmented Polyimide-Polyorganosiloxane Copolymers*, Springer Berlin Heidelberg, Berlin.

Mirjavadi, S.S., Afshari, B.M., Shafiei, N., Hamouda, A., Kazemi, M. and Structures, C. (2017a), "Thermal vibration of two-dimensional functionally graded (2D-FG) porous Timoshenko nanobeams", *Steel Compos. Struct*., **25**(4), 415-426. https://doi.org/10.12989/scs.2017.25.4.415.

Mirjavadi, S.S., Matin, A., Shafiei, N., Rabby, S. and Mohasel Afshari, B. (2017b), "Thermal buckling behavior of two-dimensional imperfect functionally graded microscale-tapered porous beam", *J. Therm. Stress*., **40**(10), 1201-1214. https://doi.org/10.1080/01495739.2017.1332962.

Mirjavadi, S.S., Rabby, S., Shafiei, N., Afshari, B.M. and Kazemi, M. (2017c), "On size-dependent free vibration and thermal buckling of axially functionally graded nanobeams in thermal environment", *Appl. Phys. A*, **123**(5), 315. https://doi.org/10.1007/s00339-017-0918-1.

Mousavi, S.M., Shafiei, N. and Dadvand, A. (2017), "Numerical simulation of subsonic turbulent flow over NACA0012 airfoil: evaluation of turbulence models", *Sigma J. Eng. Natural Sci*., **35**(1), 133-155.

Ning, F., He, G., Sheng, C., He, H., Wang, J., Zhou, R. and Ning, X. (2021), "Yarn on yarn abrasion performance of high modulus polyethylene fiber improved by graphene/polyurethane composites coating", *J. Eng. Fibers Fabrics*, **16**, 1558925020983563. https://doi.org/10.1177/1558925020983563.

Omidi, S., Oskooee, M.B. and Shafiei, N. (2013), "Finite element analysis of an ultra-fine grained Titanium dental implant covered by different thicknesses of hydroxyapatite layer", *Indian J. Dentistry*, **4**(1), 1-4.

https://doi.org/10.1016/j.ijd.2012.10.002.
Rafiee, Z. (2015), "High thermally stable and organosoluble new poly(amide-imide)s derived from bis(4-trimellitimido phenoxy) phenyl Triptycene", *J. Macromol. Sci. B*, **54**(6), 749-759. https://doi.org/10.1080/00222348.2015.1037216.
Rasheed, A. and Khalid, F.A. (2014), "Fabrication and properties of CNTs reinforced polymeric matrix nanocomposites for sports applications", *IOP Conference Series Mater. Sci. Eng.*, **60**, 012009. https://doi.org/10.1088/1757-899x/60/1/012009.
Shafiei, N., Ghadiri, M. and Mahinzare, M. (2019), "Flapwise bending vibration analysis of rotary tapered functionally graded nanobeam in thermal environment", *Mech. Adv. Mater. Struct.*, **26**(2), 139-155. https://doi.org/10.1080/15376494.2017.1365982.
Shafiei, N., Kazemi, M. and Ghadiri, M. (2016a), "Nonlinear vibration of axially functionally graded tapered microbeams", *Int. J. Eng. Sci.*, **102**, 12-26. https://doi.org/10.1016/j.ijengsci.2016.02.007.
Shafiei, N., Kazemi, M., Safi, M. and Ghadiri, M. (2016b), "Nonlinear vibration of axially functionally graded non-uniform nanobeams", *Int. J. Eng. Sci.*, **106**, 77-94. https://doi.org/10.1016/j.ijengsci.2016.05.009.
Sheng, C., He, G., Hu, Z., Chou, C., Shi, J., Li, J., Meng, Q., Ning, X., Wang, L. and Ning, F. (2021), "Yarn on yarn abrasion failure mechanism of ultrahigh molecular weight polyethylene fiber", *J. Eng. Fibers Fabrics*, **16**, 15589250211052766. https://doi.org/10.1177/15589250211052766.
Si, Z., Yang, M., Yu, Y. and Ding, T. (2021), "Photovoltaic power forecast based on satellite images considering effects of solar position", *Appl. Energy*, **302**, 117514. https://doi.org/10.1016/j.apenergy.2021.117514.
Wang, J., Long, Y., Sun, Y., Zhang, X., Yang, H. and Lin, B. (2017), "Enhanced energy density and thermostability in polyimide nanocomposites containing core-shell structured $BaTiO_3$@SiO_2 nanofibers", *Appl. Surf. Sci.*, **426**, 437-445. https://doi.org/10.1016/j.apsusc.2017.07.149.
Wang, M., Yang, M., Fang, Z., Wang, M. and Wu, Q. (2022), "A practical feeder planning model for urban distribution system", *IEEE T. Power Syst.*, 1-1. https://doi.org/10.1109/TPWRS.2022.3170933.
Zhang, H., Zhao, X., Zong, G. and Xu, N. (2022a), "Fully distributed consensus of switched heterogeneous nonlinear multi-agent systems with bouc-wen hysteresis input", *IEEE T. Netw. Sci. Eng.*, **9**(6), 4198-4208. https://doi.org/10.1109/TNSE.2022.3196316.
Zhang, J., Wang, X., Zhou, L., Liu, G., Adroja, D.T., da Silva, I., Demmel, F., Khalyavin, D., Sannigrahi, J., Nair, H.S., Duan, L., Zhao, J., Deng, Z., Yu, R., Shen, X., Yu, R., Zhao, H., Zhao, J., Long, Y., Hu, Z., Lin, H.J., Chan, T.S., Chen, C.T., Wu, W. and Jin, C. (2022b), "A ferrotoroidic candidate with well-separated spin chains", *Adv. Mater.*, **34**(12), 2106728. https://doi.org/10.1002/adma.202106728.
Zhang, Z., Yang, Q., Yu, Z., Wang, H. and Zhang, T. (2022c), "Influence of Y_2O_3 addition on the microstructure of TiC reinforced Ti-based composite coating prepared by laser cladding", *Mater. Character.*, **189**, 111962. https://doi.org/10.1016/j.matchar.2022.111962.
Zhao, J., Gao, J., Li, W., Qian, Y., Shen, X., Wang, X., Shen, X., Hu, Z., Dong, C., Huang, Q., Cao, L., Li, Z., Zhang, J., Ren, C., Duan, L., Liu, Q., Yu, R., Ren, Y., Weng, S.-C., Lin, H.-J., Chen, C.T., Tjeng, L.H., Long, Y., Deng, Z., Zhu, J., Wang, X., Weng, H., Yu, R., Greenblatt, M. and Jin, C. (2021), "A combinatory ferroelectric compound bridging simple ABO_3 and A-site-ordered quadruple perovskite", *Nature Commun.*, **12**(1), 747. https://doi.org/10.1038/s41467-020-20833-6.
Zhao, Y., Tang, F., Zong, G., Zhao, X. and Xu, N. (2022), "Event-based adaptive containment control for nonlinear multiagent systems with periodic disturbances", *IEEE T. Circ. Syst. II*, **69**(12), 5049-5053. https://doi.org/10.1109/TCSII.2022.3200053.

JL